ELSEVIER

Chemical Engineering Journal 92 (2003) 243–253

Chemical Engineering Journal

www.elsevier.com/locate/cej

On the determination of axial dispersion coefficient in a batch oscillatory baffled column using laser induced fluorescence

A.W. Fitch, X. Ni*

Department of Mechanical and Chemical Engineering, Centre for Oscillatory Baffled Reactor Applications (COBRA), Heriot-Watt University, Edinburgh EH14 4AS, UK

Abstract

We report a novel method of obtaining tracer concentration profiles and determining the axial dispersion coefficient in a batch oscillatory baffled column (OBC) utilising the laser induced fluorescence (LIF) technique. In LIF, a dye fluoresces when it is induced by a laser. By receiving the wavelength of the light emitted by the dye, the intensity of the dye can be converted into the concentration. This technique is non-intrusive and has a number of unique advantages in comparison with the traditional tracer method. One of such advantages is that it can be used to investigate the concentration profiles in different areas of the cell axially and radially, which has led to, for the first time, the quantitative determination of the radial dispersion in the OBC. In short, LIF is a viable and powerful tool in quantifying mixing and dispersion in both the OBC and other reactor systems.

Keywords: Oscillatory baffled column; Laser induced fluorescence; Mixing time; Axial dispersion coefficient; Cell residence time; Tanks-in-series-model

1. Introduction

In chemical engineering, the axial dispersion coefficient is the universal index used to describe the characteristics of mixing in both continuous and batch vessels. It is a measure of the degree of deviation in flows from the true plug flow scenario. Theoretically, the axial dispersion coefficient for a plug flow should be zero. The governing equation of the axial dispersion coefficient (E) in a continuous system without reaction is described by

$$\frac{\partial C}{\partial t} = E\left(\frac{\partial^2 C}{\partial x^2}\right) - U\left(\frac{\partial C}{\partial x}\right) \quad (1)$$

where C is the concentration of species ($g\,l^{-1}$), U the mean axial velocity of the flow ($m\,s^{-1}$), t the time (s), x the position along the axial length (m) and E the axial dispersion coefficient ($m^2\,s^{-1}$). The concept of E originated from molecular diffusion [1] and the value of which is constant throughout a given system. When dealing with batch vessels where there is no net flow, i.e. $U = 0$, thus the above equation reduces to

$$\frac{\partial C}{\partial t} = E\left(\frac{\partial^2 C}{\partial x^2}\right) \quad (2)$$

Mathematical approximations of Eq. (1) have been reported over the past 50 years [2–7]. An exact analytical solution of the partial differential equation is difficult to obtain, however, approximate mathematical solutions or numerical results are widely used together with experimental measurements of residence time distributions (RTD). For continuous systems the RTDs are obtained when a perfect or an imperfect pulsed injection of a tracer solution enters the vessel and the measuring probes located downstream to the injection (Fig. 1) register the change of the concentration of the tracer as it travels along the length of the vessel.

By reconstructing the RTD of a further downstream location, e.g. sample port 2 in Fig. 1, with an axial dispersion model (Eq. (1)) together with a RTD of a location close to the injection port, e.g. sample port 1 in Fig. 1, as an initial input, the axial dispersion coefficient can be obtained [8,9]. However, in a batch vessel the tracer concentration profiles (Fig. 2) differ significantly from that in the continuous systems. The concept of RTD does not apply here. The tracer concentration profiles shown in Fig. 2 suggest that the flow in the vessel is far from the characteristics of a plug flow. Under these circumstances, the tanks-in-series-model or tanks-in-series-with-back-mixing-model is often employed [10,11]. In the tanks-in-series-model, for instance, the volume of a vessel is subdivided into a series of compartments of an equal size. Each compartment represents a perfect mixed tank, and an inter-cell mixing flow rate (Q) flows through these compartments. Let C_n be the concentration

* Corresponding author. Tel.: +44-131-451-3781; fax: +44-131-451-3077.
E-mail address: x.ni@hw.ac.uk (X. Ni).

1385-8947/02/$ – see front matter © 2002 Elsevier Science B.V. All rights reserved.
PII: S1385-8947(02)00261-9

Nomenclature

B	dimensionless constant = 0.5
C	concentration (g dm^{-3})
D	diameter of column (m)
$D_{orifice}$	diameter of baffle orifice (m)
E	axial dispersion coefficient (m^2 s^{-1})
f	oscillation frequency (Hz)
gs	greyscale
H	dimensionless baffle spacing (L/D)
K	constant for zero greyscale
L	length between baffles (m)
m	gradient of greyscale
Q	inter-cell mixing flow rate (m^3 s^{-1})
Re_o	oscillatory Reynolds number
St	Strouhal number
t	time (s)
T_{mix}	mixing time (s)
u	net flow velocity (m s^{-1})
V	volume (m^3)
x_o	oscillating amplitude (m, centre to peak)
Z	axial length (m)

Greek symbols

α	baffle free area
μ	viscosity (kg m^{-1} s^{-1})
ρ	density (kg m^{-3})
τ_{mix}	cell residence time (s)
ω	angular frequency (=$2\pi f$)

profile measured by a probe in a cell nearer to the injection point and C_f be the concentration measured further away from the injection, as shown in Fig. 2. Using the imperfect tracer pulse method and setting a value for Q, the tracer concentrations in all the other compartments can be calculated by solving the following difference equations based on a numerical approach [11,12]:

$$C_0(0) = C_n(0), \quad t = 0 \tag{3}$$

$$C_p(0) = 0, \quad 1 \le p \le M \tag{4}$$

$$C_0(t + \Delta t) = C_n(t + \Delta t) \tag{5}$$

$$C_p(t + \Delta t) = C_p(t) + \frac{\Delta t\, Q}{V_{cell}}[C_{p-1}(t) + C_{p+1}(t) - 2C_p(t)], \quad 1 \le p \le M \tag{6}$$

$$C_M(t + \Delta t) = C_M(t) + \frac{\Delta t\, Q}{V_{cell}}[C_{M-1}(t) - C_M(t)] \tag{7}$$

where M is the total number of compartments after the first probe in relation to the tracer injection. The calculated concentration, C_{N+1}, is then compared with the experimental one, C_f, until $\sum_{t=0}^{t_\infty}[C_{N+1}(t) - C_f(t)]^2$ is minimised, where N is the number of cells between the two probes. In this way, Q can be determined. From this, a cell residence time (s), $\tau_{mix} = V_{cell}/Q$, can be obtained, which is closely related to the axial dispersion coefficient as

$$E\ (\text{m}^2\ \text{s}^{-1}) = \frac{\text{constant}}{\tau_{mix}} \tag{8}$$

It is clear that for both continuous and batch systems, experimental tracer measurements are vitally important in the determination of axial dispersion coefficient. The traditional technique involves using a salt solution as tracer and conductivity probes as the means to register the changes of the tracer concentration at a number of positions along the vessel. In this paper, we report our novel approach of applying laser induced fluorescence (LIF) to obtain such concentration profiles and of determining axial dispersion coefficient

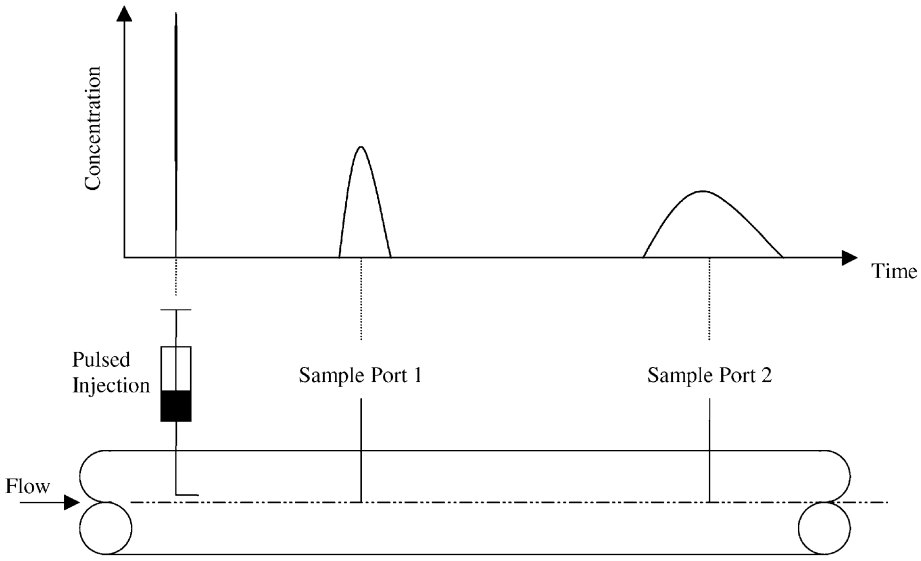

Fig. 1. Tracer experiment set-up in a continuous system.

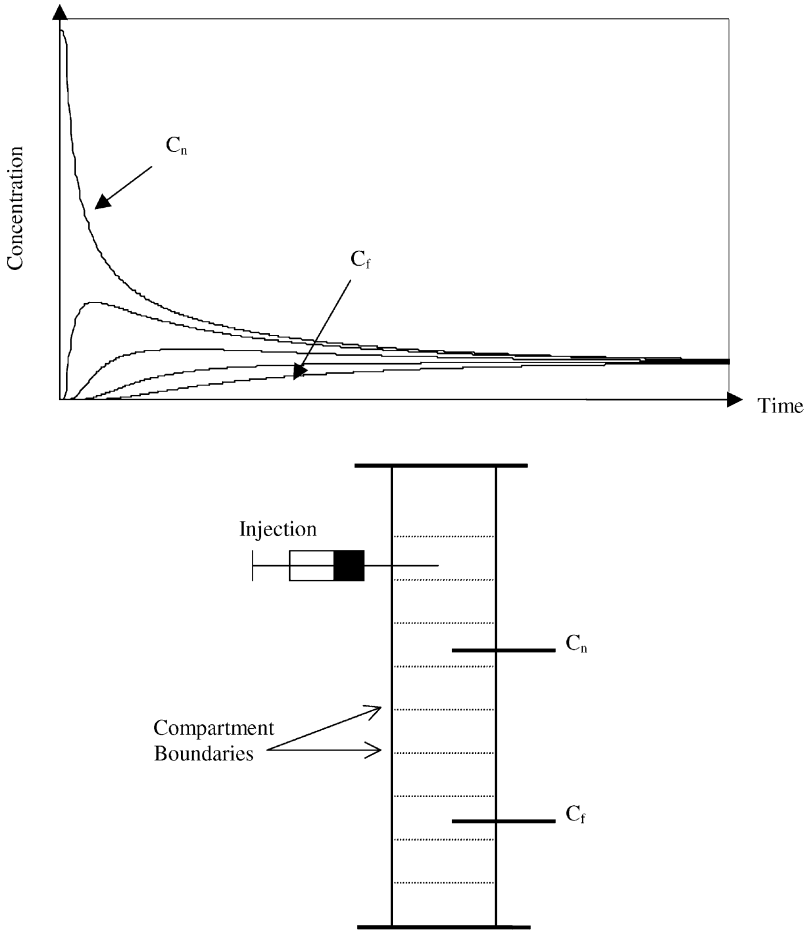

Fig. 2. Tracer experiment set-up in a batch system.

in a batch oscillatory baffled column (OBC) without involving lengthy numerical iterations.

2. Oscillatory baffled column

The OBC is a unique mixing device, and consists of a cylindrical column containing equally spaced orifice baffles and fluid oscillation can be applied at one or both ends of the vessel using bellows, piston or diaphragm. The schematic diagram of such a device is shown in Fig. 3. The mixing mechanism in an OBC can be understood with the help of Fig. 4. Fundamentally, there must be sharp edges (provided by the baffles) presented transverse to a fully reversing flow. The interactions between baffles and fluid oscillations generate significant eddy motions in both axial and radial directions, offering uniform and enhanced mixing within each baffled cavity as well as along the length of the column [8,9,13,14].

There are four dimensionless groups that govern the fluid mechanical conditions in a batch OBC: the baffle spacing ($H = L/D$), the baffle free area ($\alpha = D_{\text{orifice}}/D$), which are kept constant in this study; the oscillatory Reynolds number (Re_o) and the Strouhal number (St), which are defined as

$$Re_o = \frac{2\pi f x_o \rho D}{\mu} \tag{9}$$

$$St = \frac{D}{4\pi x_o} \tag{10}$$

where ρ is the fluid density (kg m^{-3}), D the diameter of the column (m), x_o the oscillation amplitude (m, centre to peak), ω is the angular frequency ($2\pi f$), with f being the oscillation frequency (Hz) and μ is the fluid viscosity (kg (m s)$^{-1}$). The oscillatory Reynolds number describes the intensity of mixing applied to the column, while the Strouhal number is the ratio of column diameter to stroke length, characterising the effective eddy propagation [8,10,15,16].

The batch OBC used in this study is made of a vertical Perspex tube of 500 mm in height and 50 mm in diameter with a liquid capacity of 1 l, as shown in Fig. 3. A rectangular viewing box is sealed around the tube at the point of investigation and filled with a compensating liquid to minimise refractive effects caused by wall curvature. A stainless steel bellows, linking the base of the column to the fly arm of an electric motor, drives the oscillation and the speed

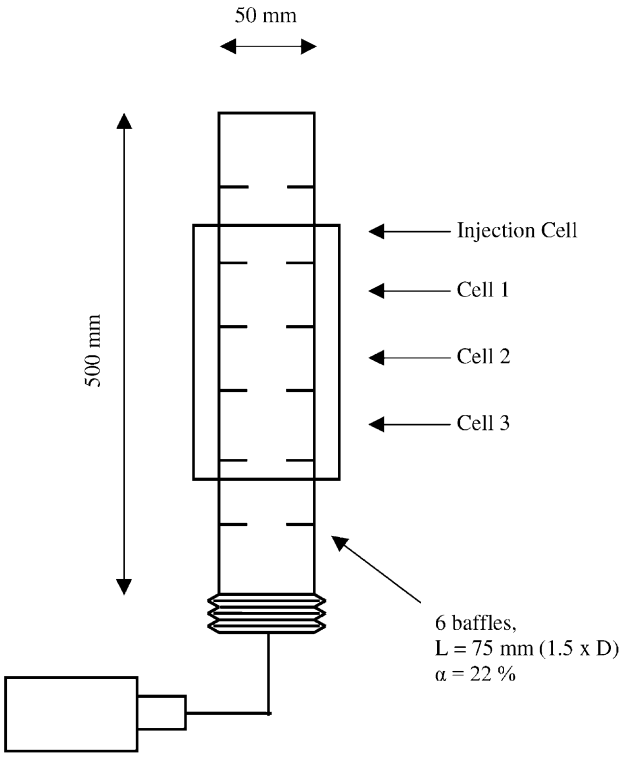

Fig. 3. An oscillatory baffled column.

of the motor provides oscillation frequencies between 0.2 and 10 Hz. The eccentric distance between the fly arm and the crank of the motor generates oscillation amplitudes of 2–8 mm (centre to peak). Affixed to the motor arm is a slotted disk that revolves with the motor through an optic pick up, which produces a pulse for every peak of oscillation. This pulse is important as it provides a mechanism to synchronise the start of oscillation with the LIF operation. Six baffles, each with a 22% baffle free area and evenly spaced at 75 mm apart, are fixed in the column by two connecting rods. The baffled cells are numbered with respect to an injection cell (see Fig. 3).

3. LIF system

The principle of LIF is that a dye fluoresces when induced by a laser. A narrow band pass filter, fitted to the camera, allows the wavelength of the light, emitted solely by the excited dye, to progress to the CCD array (film or CMOS sensor) of the camera. The intensity of fluoresced dye corresponds to a concentration, which is calibrated prior to experiments with known volumes of the dye. By the use of sequential imaging, the dispersion of the dye can be monitored and the concentration quantified.

The LIF set-up is illustrated in Fig. 5. It consists of a 4 W continuous argon-ion laser (Spectra Physics) and a light sheet generator, which converts the laser beam into a thin sheet of light by a combination of a 16-sided rotating mirror and a parabolic mirror. This 2 mm wide light sheet is directed through the centre of the OBC. A high-speed mono-coloured CCD camera (Kodak Ektapro 4540mx) is operated at a frame rate of 30 frames per second and triggered to record images at the same time as start of the oscillation. Embedded in the

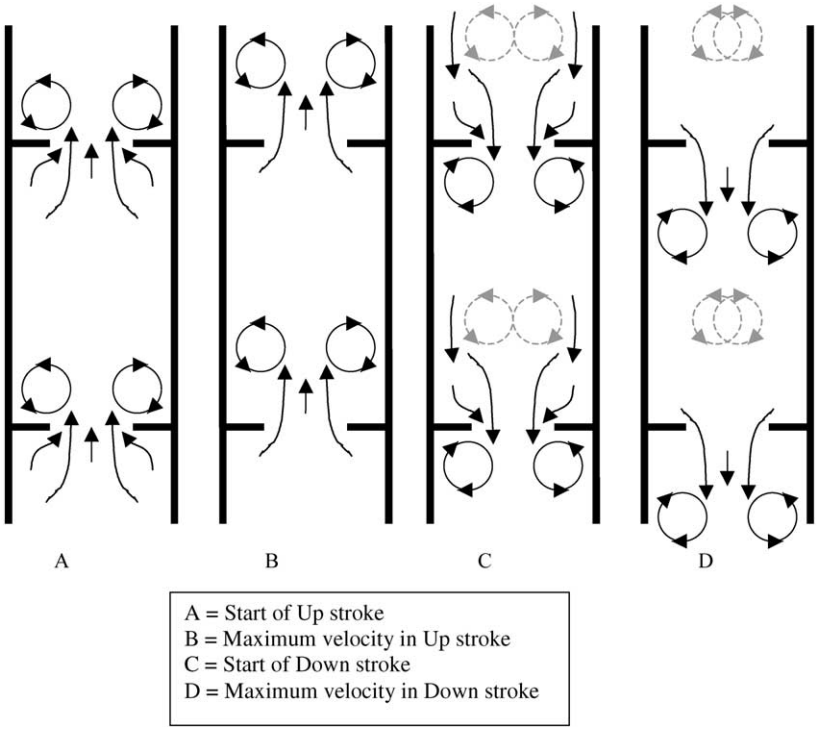

Fig. 4. Mechanism of mixing in an oscillatory baffled column.

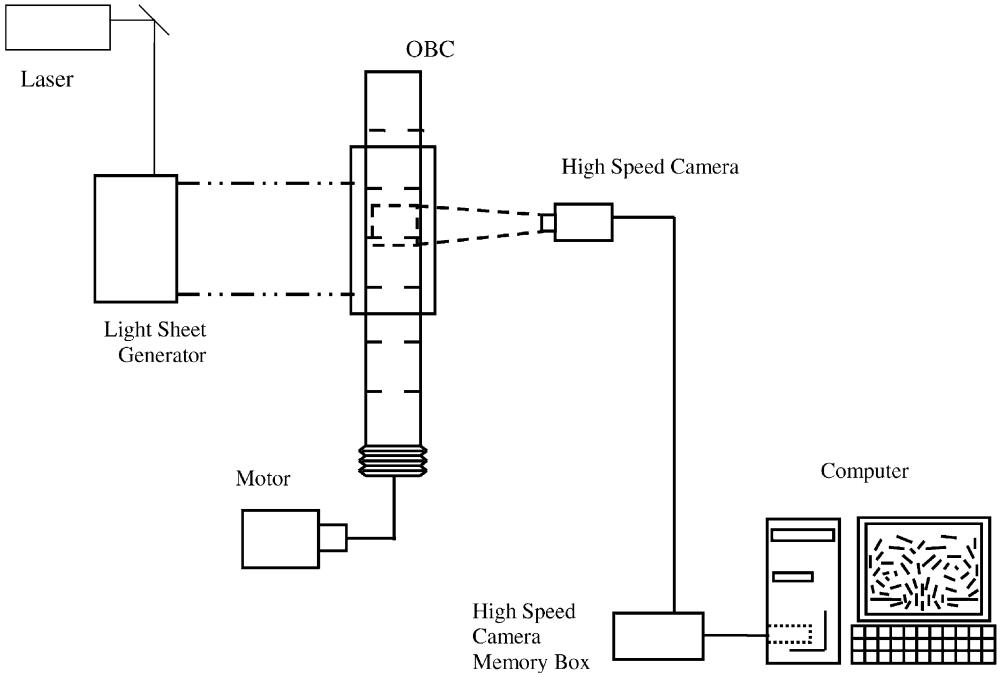

Fig. 5. A schematic diagram of OBC and LIF set-up.

C-mount of the lens is a narrow pass filter, allowing only the light of 590 nm (±5 nm) to pass. This wavelength is consistent with that of the excited dye (dye in contact with the laser). The fluorescence dye used in this study is a 1 g l^{-1} Rhodamine B solution, which is neutrally buoyant in water.

4. Experimental procedure and results

4.1. Experimental procedure

The OBC, filled with 1 l of water, is set to rest at a peak of an oscillation amplitude, while the camera is positioned and focused on a recording cell, e.g. Cell 1 in Fig. 3. One millilitre of the dye is carefully added into the injection cell, i.e. position the needle of a syringe on a baffle to counteract the down force of the injection so that the dye stratifies quickly with water until a thin layer of dye is at rest on the surface of the baffle in the injection cell. The camera and the fluid oscillations are simultaneously started (due to the synchronisation trigger attached to the motor arm), therefore, we are investigating the mixing time and axial dispersion from the start-up of the experiments. Images from the start to when the dye is of a uniform distribution within the OBC are recorded and then downloaded from the camera to a computer for analysis.

4.2. Determination of concentration profiles

Each frame in the video footage is separated into JPEG images with timing information. Fig. 6 shows a selection from a typical series of images filmed at Cell 1 in an experiment operated at $Re_o = 1250$ and $St = 1.0$ ($x_o = 4$ mm and $f = 1$ Hz), from the start ($t = 0$ s), to finish ($t = 120$ s). Each image has dimensions of 256 × 256 pixels and each pixel has a designated greyscale value between 0 and 255 (0 corresponding to black and 255 to white). A Java program designed and developed by Smith calculates the greyscale distributions shown in Fig. 7, which corresponds to the six frames in Fig. 6. The program scans each image, line by line, and passes the number of pixels corresponding to each greyscale value into a one-dimensional distribution array (0–255). It should be noted that the black edges surrounding the left, right and bottom of the images in Fig. 6a–f are removed from processing, i.e. only the images within the column area are of interest. The array is then averaged, rendering an average greyscale for that image. The greyscale is then converted, by means of a linear interpolation, to the concentration of the dye. This is done by setting the initial averaged greyscale, at $t = 0$, equivalent to a concentration ($C_{t=0}$) of 0 ml of dye per litre of water, and the final averaged greyscale, at $t = \infty$, associated with a concentration ($C_{t=\infty}$) of 1 ml of dye per litre of water

$$\overline{gs}_{t=0}\ (\text{ml dye (l water)}^{-1}) \equiv 0 \tag{11}$$

$$\overline{gs}_{t=\infty}\ (\text{ml dye (l water)}^{-1}) \equiv 1 \tag{12}$$

where gs is the greyscale (dimensionless) and t is time (s) at start (0) and finish (∞). The gradient, m, that connects the dye concentration with the greyscale is then

$$m\ (\text{ml dye (l water)}^{-1}) = \frac{C_{t=\infty} - C_{t=0}}{\overline{gs}_{t=\infty} - \overline{gs}_{t=0}} \tag{13}$$

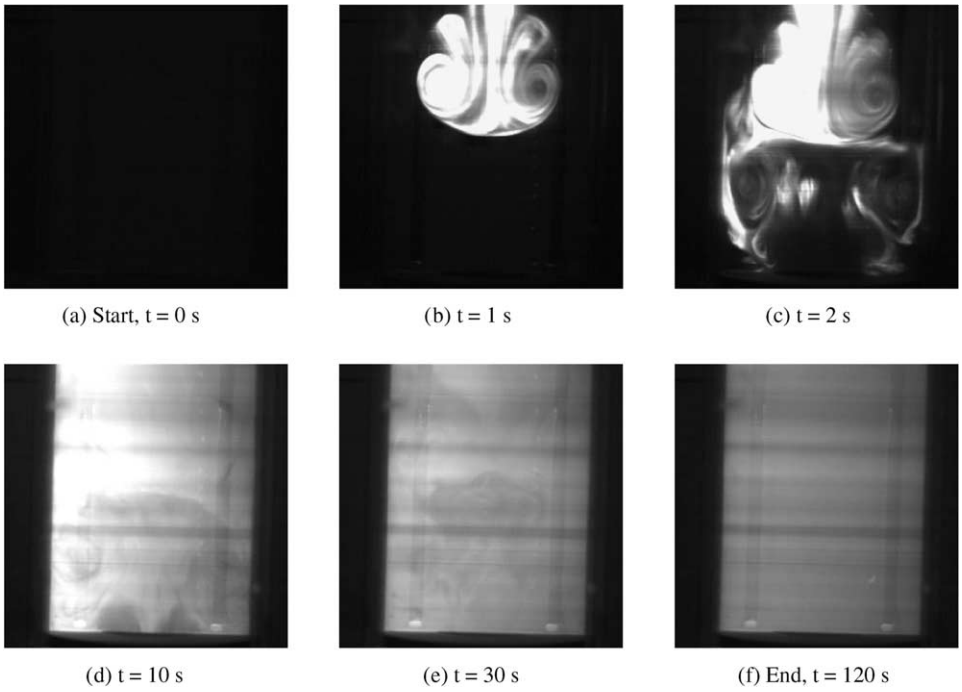

Fig. 6. Images of variations of dye with time in cell 1. $Re_o = 1250$, $St = 1.0$ ($x_o = 4\,\text{mm}$, $f = 1\,\text{Hz}$).

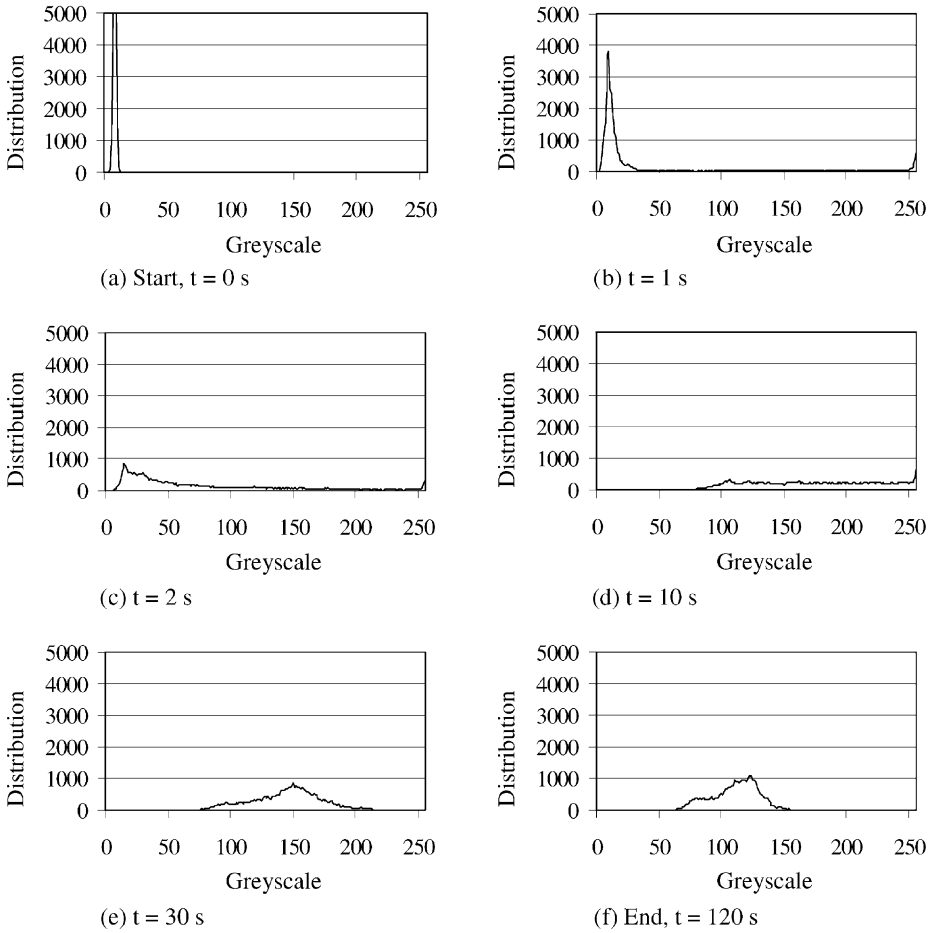

Fig. 7. Greyscale distributions corresponding to Fig. 6a–f.

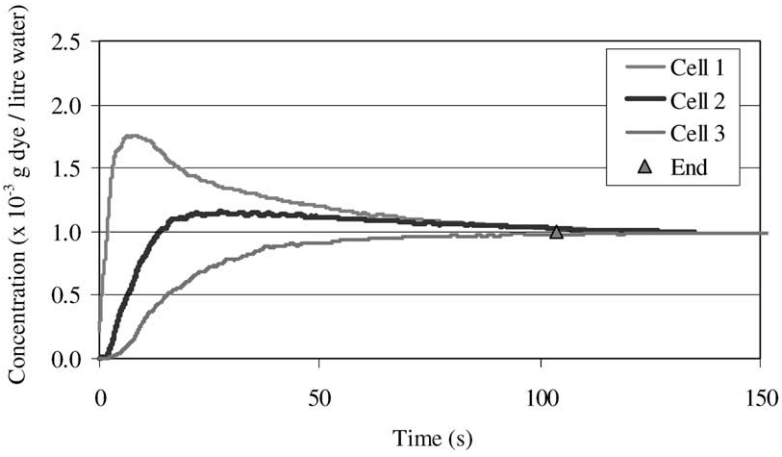

Fig. 8. Dye concentration vs. time. $Re_o = 1250$, $St = 1.0$ ($x_o = 4$ mm, $f = 1$ Hz).

The concentration intercept value (K) at a greyscale value of zero is

$$K\ (\text{ml dye (l water)}^{-1}) = -(m \times \overline{\text{gs}}_{t=0}) \tag{14}$$

Therefore, the overall concentration equation, for the ith time value of greyscale, is

$$C_{t=i}\ (\text{ml dye (l water)}^{-1}) = \left(\frac{C_{t=\infty} - C_{t=0}}{\overline{\text{gs}}_{t=\infty} - \overline{\text{gs}}_{t=0}}\right)\overline{\text{gs}}_{t=i} - \left(\frac{C_{t=\infty} - C_{t=0}}{\overline{\text{gs}}_{t=\infty} - \overline{\text{gs}}_{t=0}}\right)\overline{\text{gs}}_{t=0} \tag{15}$$

Since the overall concentration of dye injected is 1 ml of dye, then the value of $[C_{t=\infty} - C_{t=0}]$ will be 1 ml of dye per litre of water. Eq. (15) therefore reduces to

$$C_{t=i}\ (\text{ml dye (l water)}^{-1}) = \frac{\overline{\text{gs}}_{t=i} - \overline{\text{gs}}_{t=0}}{\overline{\text{gs}}_{t=\infty} - \overline{\text{gs}}_{t=0}} \tag{16}$$

i.e. the concentration is a linear function of the greyscale. The output of this equation, for a given experiment set, yields a concentration versus time distribution, similar to that obtained in the tracer and probe experiments. Fig. 8 is one of such graphs corresponding to the images and greyscale distributions previously shown in Figs. 6 and 7 for all three investigated cells in the OBC, $Re_o = 1250$, $St = 1.0$ ($x_o = 4$ mm and $f = 1$ Hz). These concentration profiles resemble remarkably those obtained using traditional tracer experiments [11,17].

With our LIF and CCD camera set-up, we can easily further divide, along the axial direction, each measuring cell into two sub-units of an equal size, as shown in Fig. 9, and five equal compartments radially, as shown in Fig. 10. In this way, we can examine the concentration profiles in detail in both directions. Figs. 11 and 12 show such information. In the axial direction, the concentration profiles share the same trend as that shown in Fig. 8, with a high degree of convergence. Furthermore, the average of the two half cell profiles (a and b) is equal to its full cell profile, i.e. (Cell 1a + Cell 1b)/2 = Cell 1. On the other hand, the radial concentration profiles within a measuring cell are almost identical (Fig. 12), indicating that the radial dispersion is uniform within an OBC. This is in fact the first positive identification on this aspect. The non-intrusive LIF technique provides a unique and powerful tool in quantifying the spatial variance

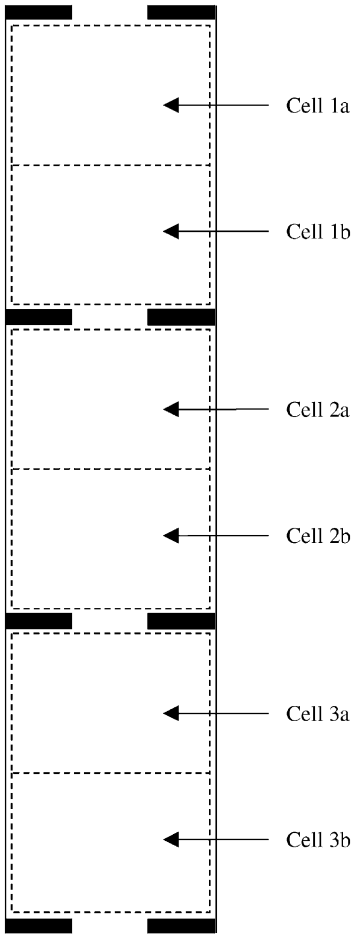

Fig. 9. Division of cell for axial inspection.

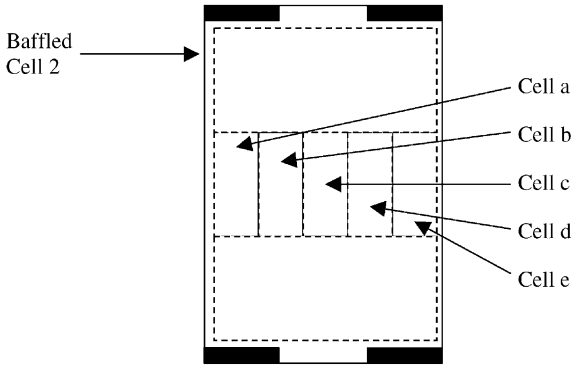

Fig. 10. Division of cell for radial inspection.

in mixing and dispersion in the OBC as well as other reactor systems. The concentration profiles shown in Figs. 11 and 12 serve an important part in understanding the characteristics of mixing in the OBC.

Notably, there will be errors in the calculation of the concentration. Measurement errors in the bulk volume and in the dye volume are around about ±2.5 and ±0.1 ml, respectively. The time between the dye injection/settlement and the motor start-up (typically around 2 or 3 s) would allow the dye to diffuse slightly by the Brownian motion, though over such a short time the effect is negligible. The distribution of the light intensity, as shown in Fig. 6 (especially b and d), is another factor, which would affect the point-measurements of the greyscale, however, as we are averaging the greyscales over the column area, the effect is decoupling and very small overall. Other experimental errors involve the measurement of the geometry (±1%) and the determination of T_{mix} (±2.5%). The combined error is about 5%.

4.3. Determination of mixing time and axial dispersion coefficient

From the concentration profiles shown in Fig. 8, it can be seen that the changes of concentration were instantly apparent in Cell 1, which is the closest cell to the cell of dye, while the changes in Cell 3 were smaller and of a much flatter slope than that in Cell 1. All three concentration curves converge to the final concentration of 1 g dye per litre of water, which is the concentration of dye used in

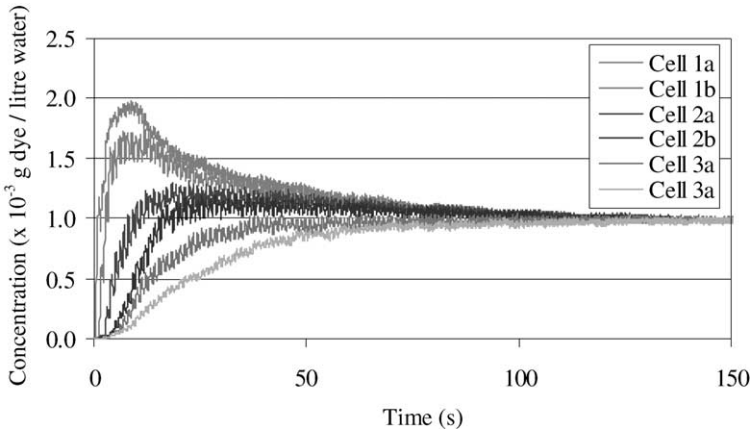

Fig. 11. Concentration vs. time along axial sub-cells. $Re_o = 1250$, $St = 1.0$ ($x_o = 4$ mm, $f = 1$ Hz).

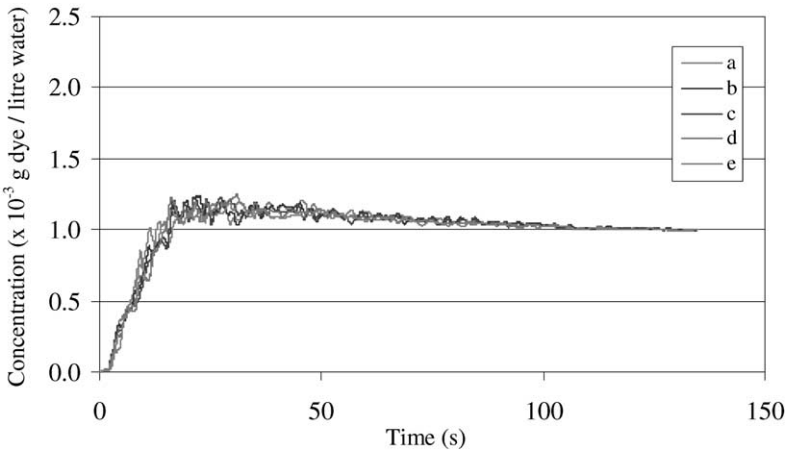

Fig. 12. Concentration vs. time across radial compartments in Cell 2. $Re_o = 1250$, $St = 1.0$ ($x_o = 4$ mm, $f = 1$ Hz).

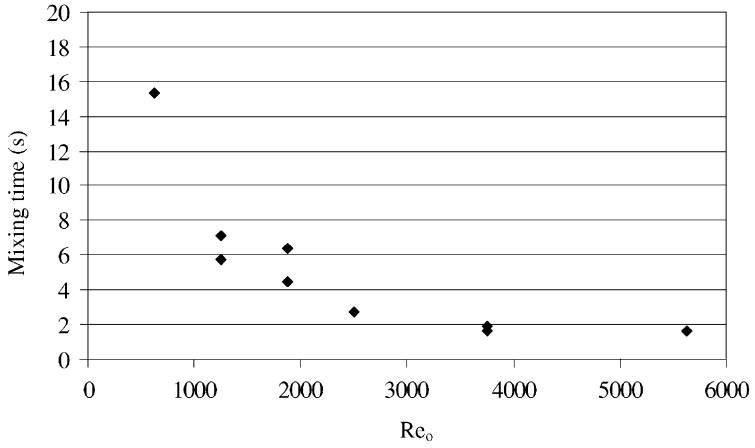

Fig. 13. Mixing time vs. oscillatory Reynolds number.

this study. If we define a mixing time (T_{mix}) as the time when the fluorescent dye was stationary at $t = 0$ to the time when a uniformity of convergence of the final concentration (±2.5%) of dye is achieved, the determination of the mixing time is then a straight forward process with a high degree of accuracy (error = 5%). We have carried out a series of LIF experiments at different oscillatory Reynolds number, the mixing time shows a decrease with the increase of Re_o (Fig. 13).

The direct determination of the overall mixing time from the concentration–time profiles allow us to evaluate the cell residence time (τ_{mix}) using the following two variables: the volume of the cell (V_{cell}) and the volume of the bulk liquid in the batch OBC (V_b). The cell residence time can be defined as

$$\tau_{mix}\,(s) = B\frac{V_{cell}}{V_b}T_{mix} \tag{17}$$

where B is a dimensionless constant equal to 0.5, taking into consideration of the movements of dye in respect to bulk liquid. Essentially, Eq. (17) divides the overall mixing time (T_{mix}) by the number of cells in the OBC (V_{cell}/V_b). Applying the τ_{mix} obtained according to Eq. (17) to the tanks-in-series-model, the concentration profiles for Cells 1–3 can readily be reconstructed. Fig. 14 shows the comparison of the concentration profiles between the modelled and experimental data. The fits are remarkably good, especially for Cells 2 and 3. There is a small over-shoot in the modelled profile of Cell 1 around 20 s into the experiment. This could be caused by the presence of high local concentrations of the dye in Cell 1, which led to a distribution of light intensity over the dye-dispersed area. However, the overall effect is small. It is clear that the direct determination of the overall mixing time with a high degree of accuracy in our LIF experiment lead to a direct establishment of τ_{mix} and subsequently the direct determination of the concentration profiles for all the baffled cells in the OBC without involving lengthy numerical iteration and minimisation.

Upon the determination of the cell residence time, τ_{mix}, the axial dispersion coefficient, E, in the batch OBC can be calculated [10]:

$$E\,(m^2\,s^{-1}) = \frac{H^2\,Re_o\,St}{2\tau_{mix}\,f}\,\frac{\mu}{\rho} \tag{18}$$

where H is the dimensionless baffle spacing. Figs. 15 and 16 show the comparison of τ_{mix} and E between the

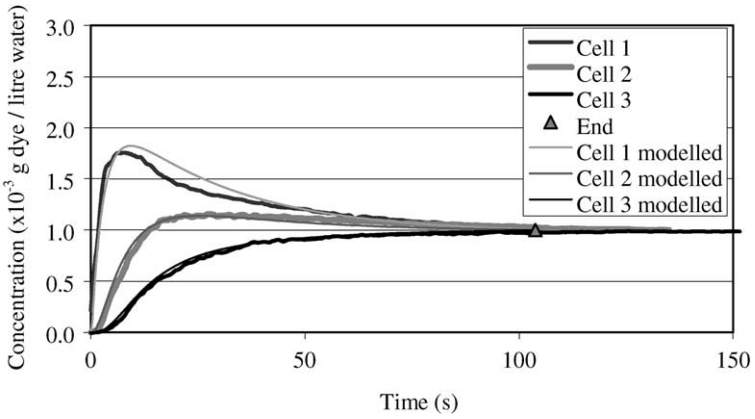

Fig. 14. Calculated and experimental concentration profiles. $Re_o = 1250$, $St = 1.0$ ($x_o = 4$ mm, $f = 1$ Hz).

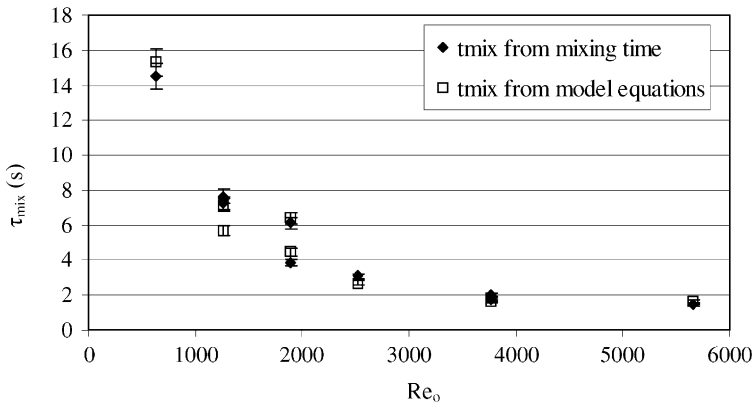

Fig. 15. Comparison of cell residence time between traditional tanks-in-series-model and our method.

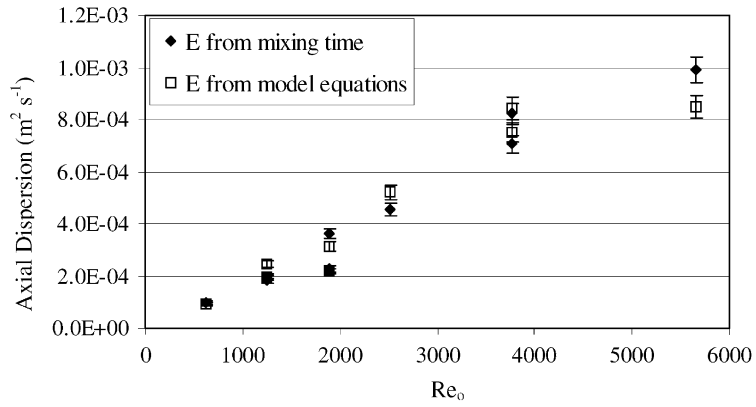

Fig. 16. Comparison of axial dispersion between traditional tanks-in-series-model and our method.

tradition approach and our direct method. A good fit can be observed in both cases.

The values of E obtained using the non-intrusive LIF technique are further compared with data reported previously in the OBC using the traditional tracer injection method [11]. The tracer used was potassium nitrite (KNO_2) in a similar OBC. The results are shown in Fig. 17. It can be seen that the evaluated axial dispersion coefficients are of a similar order of magnitude and display a similar trend for both techniques, although there are some discrepancies in data for the oscillatory Reynolds numbers of 3000–4000. These may be attributed to a number of factors and the difference in the techniques could be one of them. For the intrusive experiments, for example, the tracer is injected into a system where

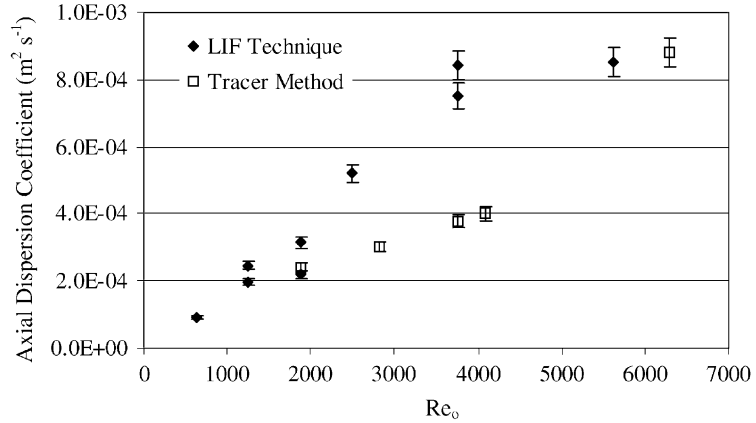

Fig. 17. Axial dispersion comparison between the traditional tracer method and the LIF technique.

the mixing has been at a steady state, while in this study the tracer is injected and set to the rest prior to the start-up of the experiments, i.e. the mixing time and axial dispersion are calculated from the start-up. Another factor is that in the intrusive experiments conductivity probes employed are usually of the membrane type, this means that the tracer has to diffuse into the membrane before registering a signal; the measurement of this sort could be less accurate than that from the non-intrusive method. With all elements considered, the two techniques still hold similar magnitudes and trends, thus the comparison suggests that the LIF method is a viable and powerful tool in the characterisation of mixing.

5. Conclusions

We have reported a novel approach of obtaining accurate concentration profiles utilising the non-intrusive LIF technique. We have shown a direct determination of the cell residence time without involving lengthy numerical iterations and minimisation. The axial dispersion coefficient determined using LIF compares closely to that obtain using the traditional tracer method.

The striking and unique advantage of using LIF is that it allows detail examination of the characteristics of mixing in both axial and radial directions easily and readily, where the traditional tracer method fails to achieve or at the expensive of using a large number of probes and lengthy experimental time. As a result, the LIF method is a powerful tool in the characteristics of mixing and dispersion.

Acknowledgements

The authors express the first acknowledgement to Cameron G. Smith who spent time writing and compiling the Java coding to convert the greyscale images to greyscale distributions. Thanks also go to EPSRC for the funding of this project.

References

[1] E.L. Cussler, Diffusion, Mass Transfer in Fluid Systems, Cambridge University Press, Cambridge, 1984.
[2] G. Taylor, Dispersion of soluble matter in a solvent flowing slowly through a tube, Proc. R. Soc. A219 (1953) 186–203.
[3] R. Aris, On the dispersion of a solute in a fluid flowing through a tube, Proc. R. Soc. A235 (1956) 67–77.
[4] O. Levenspiel, K.W. Smith, Notes on the diffusion-type model for the longitudinal mixing of fluids in flow, Chem. Eng. Sci. 6 (1957) 227–233.
[5] W.W. Gill, A note on the solution of transient dispersion problems, Proc. R. Soc. A298 (1967) 335–339.
[6] J.S. Yu, Dispersion in laminar flow through tubes by simultaneous diffusion and convection, J. Appl. Mech. 48 (1981) 217–222.
[7] J.S. Vrentas, C.W. Vrentas, Dispersion in laminar tube flow at low peclet numbers or short times, AIChE J. 34 (1988) 1423–1430.
[8] M.R. Mackley, X. Ni, Mixing and dispersion in a baffled tube for steady laminar and pulsatile flow, Chem. Eng. Sci. 46 (1991) 3139–3151.
[9] M.R. Mackley, X. Ni, Experimental fluid dispersion measurements in periodic baffled tube arrays, Chem. Eng. Sci. 48 (1993) 3293–3305.
[10] T. Howes, On the dispersion of unsteady flow in baffled tubes, Ph.D. thesis, The University of Cambridge, 1988.
[11] X. Ni, Y.G.J. Sommer de Gelicourt, J. Neil, T. Howes, On the effect of tracer density on axial dispersion in a batch oscillatory baffled column, Chem. Eng. Sci. 85 (2002) 17–25.
[12] J.C. Mecklenburgh, S. Hartland, The Theory of Backmixing, Wiley, London, 1975, ISBN 0471 59023 1.
[13] C.R. Brunold, J.C.B. Hunns, M.R. Mackley, J.W. Thompson, Experimental observations on flow patterns and energy losses for oscillatory flow in ducts containing sharp edges, Chem. Eng. Sci. 44 (1989) 1227–1244.
[14] A.W. Dickens, M.R. Mackley, H.R. Williams, Experimental residence time distribution measurements for unsteady flow in baffled tubes, Chem. Eng. Sci. 44 (1989) 1471–1479.
[15] X. Ni, P. Gough, On the discussion of the dimensionless groups governing oscillatory flow in a baffled tube, Chem. Eng. Sci. 52 (1997) 3209–3212.
[16] X. Ni, G. Brogan, A. Struthers, D.C. Bennett, S.F. Wilson, A systematic study of the effect of geometrical parameter on the mixing time in oscillatory baffled columns, Trans. IChemE 76 (A) (1998) 635–642.
[17] Y.G.J. Sommer de Gelicourt, On single phase axial dispersion in oscillatory baffled columns, M.Phil. thesis, Heriot-Watt University, 2000.